STP 1642, 2023 / available online at www.astm.org / doi: 10.1520/STP164220210104

Laura E. Hasburgh,[1] Nathan J. Bechle,[2]
and Nayomi Z. Plaza[3]

Two Proof-of-Concept, Nontraditional Density Measurement Techniques for Partially Charred Wood

Citation

L. E. Hasburgh, N. J. Bechle, and N. Z. Plaza, "Two Proof-of-Concept, Nontraditional Density Measurement Techniques for Partially Charred Wood," in *Obtaining Data for Fire Growth Models*, ed. M. C. Bruns and M. L. Janssens (West Conshohocken, PA: ASTM International, 2023), 97–107. http://doi.org/10.1520/STP164220210104[4]

ABSTRACT

As wood is exposed to high temperatures, pyrolysis begins, permanently altering the material properties as volatiles and char are formed. The rate at which char is formed is used to predict failure times for timber members and has been shown to be inversely related to the density of the wood. Because the density is a function of local exposure temperatures, it is inherently difficult to measure and typically is simplified to a single bulk value for either unmodified wood or the density of wood and char. Here, we report the use of two fast, simple density measurement techniques to characterize the changes in density in partially charred wood. The validation of these techniques will allow for more accurate density values to be obtained and included when modeling pyrolysis in wood.

Keywords

wood density, pyrolysis, thermal neutron scattering, X-ray computerized tomography

Manuscript received November 12, 2021; accepted for publication January 31, 2022.

[1]Building and Fire Sciences, U.S. Forest Products Laboratory, 1 Gifford Pinchot Dr., Madison, WI 53726, USA http://orcid.org/0000-0001-6637-2665

[2]Engineering Mechanics and Remote Sensing Lab, U.S. Forest Products Laboratory, 1 Gifford Pinchot Dr., Madison, WI 53726, USA http://orcid.org/0000-0001-5718-0493

[3]Forest Biopolymer Science and Engineering, U.S. Forest Products Laboratory, 1 Gifford Pinchot Dr., Madison, WI 53726, USA http://orcid.org/0000-0002-5198-4877

[4]ASTM 42nd Symposium on *Obtaining Data for Fire Growth Models* held virtually on December 14–15, 2021.

Introduction

Pyrolysis is the thermal degradation of organic materials that results in the release of volatiles and the formation of char. Char is the solid, carbonaceous material that remains after the wood has been exposed to high temperatures and, for engineering analyses, char forms at a temperature of 288°C or 300°C.[1–3] The role pyrolysis plays in the combustion of wood has led to the development of computational models to predict both pyrolysis and fire resistance of wood assemblies exposed to various fire conditions.[4] Over the past four decades, the capabilities of these models have seen significant advances. As both Sinha[4] and Janssens[5] have pointed out, however, because pyrolysis involves a complex series of reactions, obtaining material properties is inherently difficult.

Lautenberger, Rein, and Fernandez-Pello noted that at least eight material properties are needed to simulate pyrolysis in charring materials: thermal conductivity of the virgin fuel (k_v), specific heat of the virgin fuel (c_{pv}), pre-exponential factor (A), activation energy (E_a), heat of pyrolysis (ΔH_p), char thermal conductivity (k_c), char specific heat (c_{pc}), and char density (ρ_c).[6] Pyrolysis of wood often leads to combustion and then the processes occur simultaneously. The rate of combustion has been shown to be a function of density, permeability along the grain, moisture content, and char thickness, and the formation of decomposition products has been found to be a function of temperature, wood species, and density.[7] Of these, density is the common material property that affects pyrolysis, combustion rates, and decomposition products. Additionally, it is widely accepted that, with increasing density, the rate at which a char front propagates into solid wood decreases,[3,8–15] whereas the mass loss increases.[16–18]

Wood density is extremely variable between species and can even vary within a cross-section of a single tree. Additionally, while undergoing pyrolysis, the density of wood constantly changes as a function of local temperature. Because of the variability and the difficulty in obtaining density at high temperatures, or while undergoing active combustion, many models are simplified. Some models simplify this by using a constant that is representative of the wood,[5] a linear function in the pyrolysis region bound by the char and virgin wood values,[19,20] or the bulk density of specific condensed phase species (i.e., wet wood, dry wood, char, ash).[21]

The apparent density is obtained by dividing the oven-dry mass of a specimen by the gross volume of the specimen determined at atmospheric pressure. For more accurate measurements of density, known as real density, the oven-dry mass will be divided by the gross volume obtained through the displacement of a gas or fluid.[22] Neither method, however, can be used to determine the density across the pyrolysis zone in situ.

More recently, Friquin[7] noted that a database of wood properties, including density, would be a useful tool for fire safety engineers designing timber structures, and Naser[23] made a case for the use of artificial intelligence to derive a universal model that represents how each property changes under elevated temperature.

More recently, various techniques have been used to evaluate wood properties. X-ray computerized tomography (XCT) has been used to track changes in specific gravity due to decay[24,25] and to assess adhesive bondlines,[26] and neutron imaging (NI) has been used to measure densities across tree rings.[27] Ossler et al. revealed that the attenuation coefficient of wood using NI decreases during pyrolysis, and this change was attributed to a loss in the material's hydrogen content.[28] Ossler et al. also showed that by combining XCT with NI, the spatial resolution could be improved and used to track changes in the hydrogen content of various lignocellulosic sources as they were pyrolyzed (from room temperature to 1,000°C).[29] Neither XCT nor NI, however, have been used to measure densities across pyrolysis zones. Here, we apply these two nontraditional techniques to obtain the density through a gradient of partially charred wood to determine its applicability for future investigations that then can be applied to a universal model or database of material properties.

Methods and Materials

MATERIALS

NI was limited to specimens with dimensions less than 35 by 43 cm, whereas XCT could accommodate much larger specimens (on the order of centimeters to meters). Thus, given the differences in specimen sizes that could be evaluated by each instrument, different specimens were used (the specimen preparation details for each are provided next).

The development of the partially charred NI specimen is summarized here and further details are available in Hasburgh.[30] Before charring, Douglas-fir (*Pseudotsuga menziesii*) lumber with dimensions of 100 mm 100 mm 20 mm was dried in an oven at 105°C for 24 hours. The radial-longitudinal surface of the wood was exposed to a constant heat flux of 50 kW/m^2 using a cone calorimeter (FTT iCone Mini, East Grinstead, West Sussex, UK). The thermal profile of the specimen thickness was monitored using six thermocouples. Four duplex 30 AWG (0.25 mm diameter) Type K thermocouples, insulated with Kapton, PFA, Glass Braid Insulation (Omega Engineering, GG-K-30-SLE) were inserted into the holes parallel to the isotherm. The holes had a diameter of 0.2 mm and a length of 30 mm and were drilled in the middle of each edge of the specimen at 4 mm, 8 mm, 12 mm, or 16 mm from the unexposed surface. One additional thermocouple was on the unexposed surface and one on the top of the exposed surface of the specimen. To install the surface thermocouples, shallow notches were made using a straight blade in the center of each surface with the welded beads of the thermocouples inserted into the shallow notch. The exposure was terminated when the unexposed surface reached a temperature of 100°C. A 4-mm-thick slice from the center of the charred Douglas fir, with a gradient and known temperature profile (**fig. 1**), was obtained for analysis with NI.

For the XCT scans, the Douglas-fir specimen was constructed from lumber with a cross-section of approximately 83 mm by 83 mm. To monitor the thermal

FIG. 1 (*A*) Douglas-fir specimen for NI and (*B*) the corresponding thermal profile from measured temperatures.

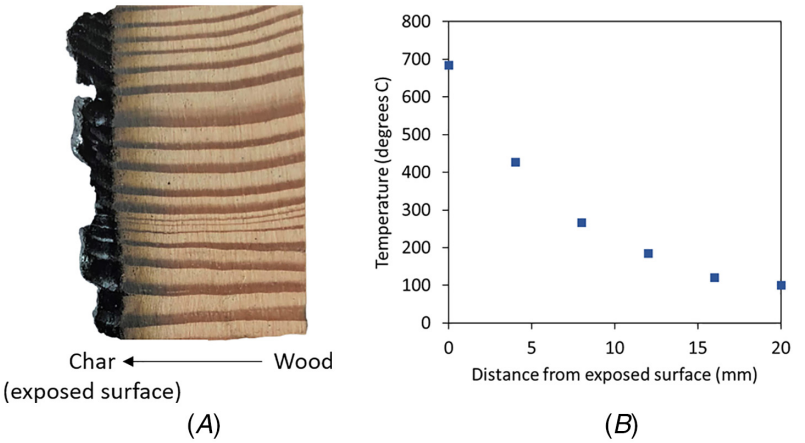

profile (**fig. 2**) during exposure to the ASTM E119, *Standard Test Methods for Fire Tests of Building Construction and Materials*, time-temperature curve, 20 duplex 30 AWG (0.25-mm diameter) type K thermocouples, insulated with Kapton, PFA, Glass Braid Insulation (Omega GG-K-30-SLE), were installed parallel to the isotherm at various depths from the exposed surface.[31] To install the surface thermocouples, shallow notches were made using a straight blade in the center of each

FIG. 2 (*A*) Douglas-fir specimen for XCT and (*B*) the corresponding final thermal profile showing the measured temperatures.

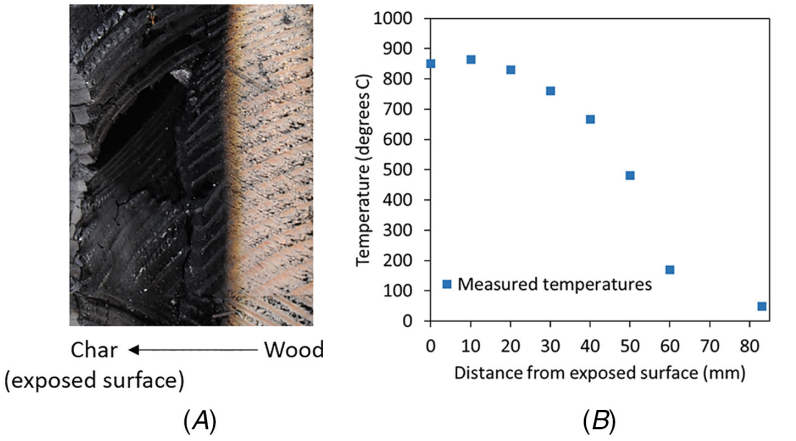

surface, the welded beads were placed in a shallow notch, and staples were used to hold the surface thermocouple in place. One thermocouple was installed on the exposed and unexposed surfaces and three thermocouples at depths of 10, 20, 30, 40, 50, and 60 mm from the exposed surface. After installation of thermocouples, the lumber was glued with a phenol-resorcinol-formaldehyde (PRF) adhesive (Hexion Cascophen LT-75 with Cascoset FM-282). The completed specimens had a final exposed surface dimension of 412 mm by 412 mm. Further details on specimen preparation can be found in Hasburgh et al.[32] In addition to the Douglas-fir specimen, a series of reference wood blocks used to relate pixel brightness to specific gravity[25] were also measured.

NEUTRON IMAGING

Douglas-fir specimens were imaged at a neutron beamline located at the Phoenix Neutron Imaging Center in Fitchburg, WI. All specimens were imaged at ambient conditions. The specimens were fastened onto aluminum plates and exposed to neutrons for about 1.5 hours. The attenuated neutron beam was measured using conventional X-ray films in contact with high-resolution neutron conversion screens. The films were developed in a dark room and digitized for quantitative analysis in FIJI, an open-source image processing software package.[33] First, the images were flattened along the *z*-axis. Then, linear profiles were drawn over several growth rings (at least five) to obtain the mean gray values across the thermal degradation profile and to calculate the macroscopic neutron attenuation coefficient based on Beer-Lambert's law, as in equation (1):

$$\Sigma = \frac{\ln \frac{I_0}{I}}{d}, \tag{1}$$

where:

I_0 = the incident beam intensity,
I = the transmitted beam intensity, and
d = the specimen thickness.

Because the attenuation coefficient depends on the number density N, and microscopic scattering cross-section (σ) of the elements present in the specimen, the measured attenuation coefficient Σ_{eff} can be described as follows:

$$\Sigma_{\text{eff}} = \sum_i^n N_I \sigma_i, \tag{2}$$

By defining the number density as:

$$N_i = \frac{\rho_i}{M_i} N_A, \tag{3}$$

where:

ρ = the material apparent density (g/cm^3),
N_A = Avogadro's constant, and
M = the atomic weight (g/mol).

Taking into account the elemental composition of dry wood (approximately 50%C, 6%H, and 44%O), and the known σ of each element, we calculated the density wood across the thermal degradation profile as follows:

$$\rho = \frac{\Sigma_{eff}}{N_A \quad 0.5\frac{\sigma_c}{M_C} + 0.44\frac{\sigma_O}{M_O} + 0.06\frac{\sigma_H}{M_H}} (\mathrm{g/cm^3}). \tag{4}$$

This approach was used to measure the apparent density across three rings in sound wood using x-ray densitometry and neutron radiography.[27] Even though, the elemental composition of the lignocellulosic material may vary during pyrolysis, the content of hydrogen, which is the major contributor to the attenuation in NI, is relatively constant below 400°C.[34] Thus, within the temperature range studied in this work, we used the elemental composition of dry wood to retrieve the density.

X-RAY COMPUTERIZED TOMOGRAPHY

XCT is a technique commonly used within the field of medicine to provide spatial representations of relative radiodensity within a substrate. Several two-dimensional X-ray scans, referred to as slices, are stacked together to construct volumetric radiodensity intensities. The XCT specimens were scanned using a General Electric LightSpeed Ultra 8 Slice helical XCT scanner at the University of Wisconsin–Madison, School of Veterinary Medicine. XCT data consist of pixel intensities in Hounsfield radiodensity units, which were transformed into density using 24 reference wood blocks of known density verified for 12% moisture content. The XCT was run with the specimens exposed to ambient condition.

Results and Discussion

The initial images obtained with both NI and XCT are provided in **figure *3A*** and ***3B***. The intensity variations across the thermal degradation profile of individual latewood (LW) and earlywood (EW) bands were then evaluated (**fig. *3C***). With its enhanced hydrogen sensitivity, NI revealed variations across the charred zone that are indistinguishable in XCT. This result suggests that combining both techniques can overall improve the spatial resolution and contrast, allowing us to measure the change in density across the pyrolysis zone by deconvoluting the effects of hydrogen loss and density changes on the neutron attenuation.

Using NI, we were able to detect gradual changes in the attenuation that were not observed in the XCT. Considering that the hydrogen loss below 400°C should be minimal,[28,34] changes observed in the attenuation of the image likely are caused by local variations in the material density linked to the thermal degradation of the wood polymers occurring between 200°C and 450°C. Thus, using equation (3), we retrieved the apparent density of the wood across the thermal degradation profile.

The results from the intensity variations along designated contours of LW and EW show a nonlinear decrease in density through the char layer and an abrupt

FIG. 3 (*A*) Digitized neutron radiograph, (*B*) raw XCT slide and, (*C*) XCT density contour map, and (*D*) measured densities in four LW bands and three EW bands for a representative specimen of Douglas-fir subjected to ASTM E119 fire exposure.

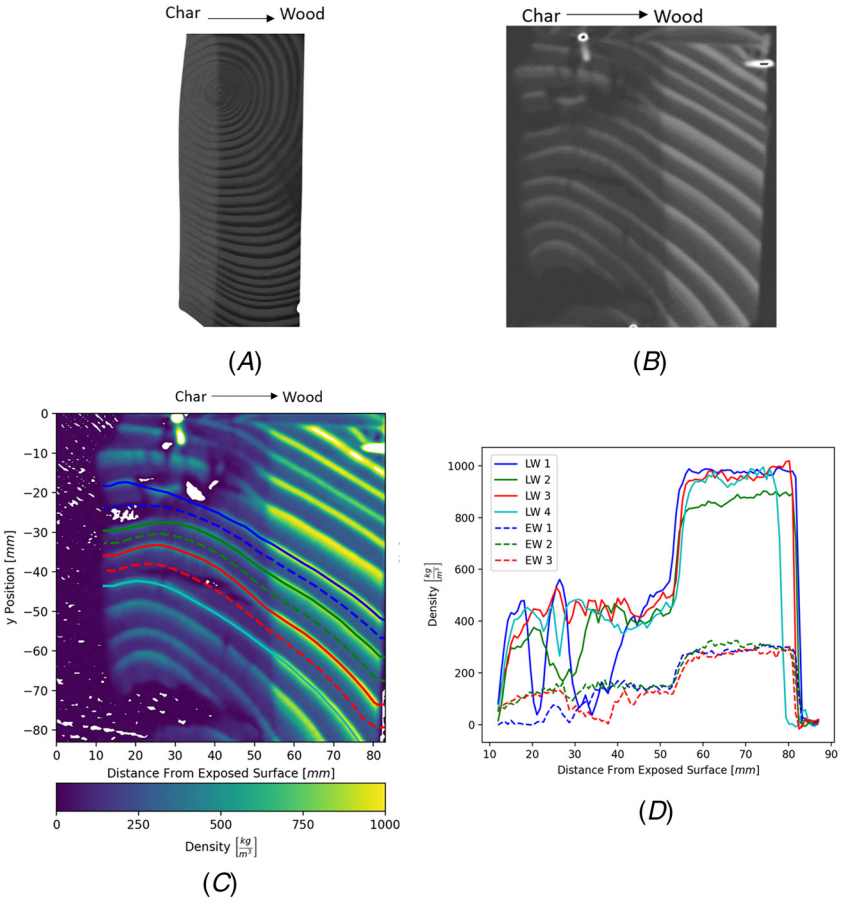

change at the transition from sound wood to charred wood (fig. 4). The percent change in density was calculated as the loss in density between the virgin wood and the char (table 1). The lesser percentage change observed in NI of EW might be attributed to its larger content of lignin. The results from both techniques are comparable and provide new insights into the density gradient across a pyrolysis-induced gradient from virgin wood to the char. Considering that the samples were imaged at ambient conditions in which the less degraded polymers may have had larger amounts of moisture, it is conceivable that the differences observed with NI below 150°C are caused by local variations in the moisture content of the wood.

FIG. 4 Changes in density as a function of maximum temperature at that location in LW and EW for both the NI and XCT specimens.

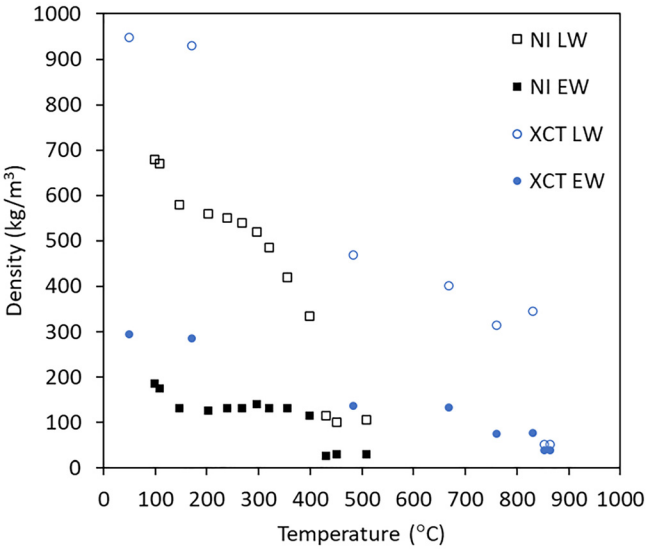

TABLE 1 Calculated density and percent changes for each technique

	Density, kg/m^3		Percent Density Change	
	XCT	NI	XCT	NI
Latewood	940 +/ 50 (V) 380 +/ 80 (C)	680 +/ 0.10 (V) 340 +/ 0.10 (C)	59.2%	50.7%
Earlywood	290 +/ 20 (V) 120 +/ 40 (C)	190 +/ 0.10 (V) 120 +/ 0.10 (C)	59.5%	35%

Note: V = virgin wood; C = char; XCT = X-ray computerized tomography; NI = neutron imaging.

The retrieved density values from XCT and NI for sound wood are comparable to those reported for EQ and LW of black spruce and jack pine, which typically vary between 550 and 700 kg/m^3 for black spruce LW, and around 300 to 450 kg/m^3 for EW.[35] Because large variability has been reported between the densities of different growth rings within a single specimen, the difference observed in the absolute values measured independently through XCT and NI are likely because different specimens were measured with each technique.

Because contrast in XCT relies on changes in electronic structure, whereas NI is susceptible to variations in hydrogen content, by combining these two techniques we could deconvolute the role of hydrogen content and local density variations in

the thermal degradation of wood. XCT, however, is much more easily accessible and capable of determining with great accuracy the overall percent density change between sound wood and charred wood.

Conclusions

Although techniques such as X-ray densitometry exist as well as other methods that can allow to determine with ease the density of wood, the two techniques presented in this manuscript have the advantage of detecting density variations in situ with minimal specimen preparation. Furthermore, by using contrast variation in NI, we could further to deconvolute the role of the different wood polymers in the observed changes in the attenuation.

These results suggest that both NI and XCT can be used to obtain density changes in charred wood that can then be implemented in pyrolysis models. Moreover, by combining the hydrogen sensitivity of NI with the well-established XCT densitometry analysis, we can further deconvolute the role of hydrogen loss and density of the individual polymers on char formation in wood.

Future work could focus on using these techniques to study active pyrolysis of wood and other model systems below 400°C. Additionally, studying pyrolyzed model material could help determine the contributions of each one of the wood polymers to the overall local density variations.

ACKNOWLEDGMENTS

The authors would like to thank Michael Taylor at the Phoenix Neutron Imaging Center and Kimberly Legler at the University of Wisconsin–Madison Veterinary Care for assisting with NI and XCT, respectively.

References

1. G. McNaughton, "Ignition and Charring Temperature of Wood: The Importance of Time in the Effect of Heat Upon Wood" (Madison, WI: U.S. Department of Agriculture, Forest Service, Forest Products Laboratory, 1944).
2. E. Schaffer, *Review of Information Related to the Charring Rate of Wood*, Report No. FPL-0145, (Madison, WI: U.S. Department of Agriculture, Forest Service, Forest Products Laboratory, 1966).
3. R. H. White, "Charring Rates of Different Wood Species" (PhD diss., University of Wisconsin–Madison, 1988).
4. S. Sinha, A. Jhalani, M. R. Ravi, and A. Ray, "Modelling of Pyrolysis in Wood: A Review," *SESI Journal* 10, no. 1 (2000): 41–62.
5. M. L. Janssens, "Modeling of the Thermal Degradation of Structural Wood Members Exposed to Fire," *Fire and Materials* 28, nos. 2-4 (2004): 199–207.
6. C. Lautenberger, G. Rein, and C. Fernandez-Pello, "The Application of a Genetic Algorithm to Estimate Material Properties for Fire Modeling from Bench-Scale Fire Test Data," *Fire Safety Journal* 41, no. 3 (2006): 204–214.

7. K. L. Friquin, "Material Properties and External Factors Influencing the Charring Rate of Solid Wood and Glue-Laminated Timber," *Fire and Materials* 35, no. 5 (2011): 303–327.
8. E. Schaffer, *Charring Rate of Selected Woods—Traverse to Grain*, Report No. FPL-69 (Madison, WI: U.S. Department of Agriculture, Forest Service, Forest Products Laboratory, 1967).
9. E. Mikkola, "Charring of Wood," in *Fire Safety Science—Proceedings of the Third International Symposium*, ed. G. Cox and B. Langford (New York, NY: Elsevier Science, 2006), 547–556.
10. R. H. White and E. V. Nordheim, "Charring Rate of Wood for ASTM E119 Exposure," *Fire Technololgy* 28, no. 1 (1992): 5–30.
11. A. H. Buchanan and A. K. Abu, *Structural Design for Fire Safety* (Chichester, UK: Wiley, 2017).
12. S. Hadvig, *Charring of Wood in Building Fires* (Lyngby, Denmark: Technical University of Denmark Press, 1981).
13. J. M. Njankouo, J.-C. Dotreppe, and J.-M. Franssen, "Experimental Study of the Charring Rate of Tropical Hardwoods," *Fire and Materials* 28, no. 1 (2004): 15–24.
14. M. Cedering, "Effect on the Charring Rate of Wood in Fire Due to Oxygen Content, Moisture Content and Wood Density" (paper presentation, Fourth International Workshop on Structures in Fire, Universidade de Averio, Averio, Portugal, May 10–12, 2006).
15. T. Harada, "Charring of Wood with Thermal Radiation, 2: Charring Rate Calculated from Mass Loss Rate," *Mokuzai Gakkai-Shi* 42, no. 2 (1996): 194–201.
16. M. Janssens, "Thermo-Physical Properties for Wood Pyrolysis Models" (paper presentation, Pacific Timber Engineering Conference, Gold Coast, Australia, July 11–15, 1994).
17. M. Janssens, "Fundamental Thermophysical Characteristics of Wood and Their Role in Enclosure Fire Growth" (PhD diss., Ghent University, 1991).
18. B. Fredlund, "A Model for Heat and Mass Transfer in Timber Structures during Fire: A Theoretical, Numerical and Experimental Study" (PhD diss., University of Lund, 1988).
19. E. J. Kansa, H. E. Perlee, and R. F. Chaiken, "Mathematical Model of Wood Pyrolysis Including Internal Forced Convection," *Combustion and Flame* 29 (1977): 311–324.
20. B. Fredlund, "Modelling of Heat and Mass Transfer in Wood Structures during Fire," *Fire Safety Journal* 20, no. 1 (1993): 39–69.
21. C. Lautenberger and C. Fernandez-Pello, "A Model for the Oxidative Pyrolysis of Wood," *Combustion and Flame* 156, no. 8 (2009): 1503–1513.
22. B. E. Cutter and E. A. McGinnes, "A Note on Density Change Patterns in Charred Wood," *Wood and Fiber Science* 13, no. 1 (1981): 39–44.
23. M. Naser, "Fire Resistance Evaluation through Artificial Intelligence: A Case for Timber Structures," *Fire Safety Journal* 105 (2019): 1–18.
24. M. McGovern, A. Senalik, G. Chen, F. C. Beall, and H. Reis, "Detection and Assessment of Wood Decay Using X-Ray Computer Tomography," *Proceedings SPIE 7647: Sensors and Smart Structures Technologies for Civil, Mechanical, and Aerospace Systems* 76474B (April 1, 2010), https://doi.org/10.1117/12.843709
25. C. A. Senalik, J. Wacker, X. Wang, and X. Wu, *Identifying Incipient Decay in Douglas-Fir Bridge Components Using X-Ray Computerized Tomography*, General Technical Report no. FPL-GTR-272, (Madison, WI: U.S. Department of Agriculture, Forest Service, Forest Products Laboratory, 2019).
26. J. L. Paris, F. A. Kamke, and X. Xiao, "X-Ray Computed Tomography of Wood-Adhesive Bondlines: Attenuation and Phase-Contrast Effects," *Wood Science and Technology* 49, no. 6 (2015): 1185–1208.
27. D. Mannes, E. Lehmann, P. Cherubini, and P. Niemz, "Neutron Imaging versus Standard X-Ray Densitometry as Method to Measure Tree-Ring Wood Density," *Trees* 21, no. 6 (2007): 605–612.

28. F. Ossler, L. J. Santodonato, J. M. Warren, C. E. A. Finney, J.-C. Bilheux, R. A. Mills, H. D. Skorpenske, and H. Z. Bilheux, "In Situ Monitoring of Hydrogen Loss during Pyrolysis of Wood by Neutron Imaging," *Proceedings of the Combustion Institute* 37, no. 2 (2019): 1273–1280.
29. F. Ossler, C. E. A. Finney, J. M. Warren, J.-C. Bilheux, Y. Zhang, R. A. Mills, L. J. Santodonato, and H. Z. Bilheux, "Dynamics of Hydrogen Loss and Structural Changes in Pyrolyzing Biomass Utilizing Neutron Imaging," *Carbon* 176 (2021): 511–529.
30. L. E. Hasburgh, "Chemical and Mechanical Characterization of Pyrolysis in Wood" (PhD diss., University of Wisconsin-Madison, 2020).
31. *Standard Test Methods for Fire Tests of Building Construction and Materials*, ASTM E119-20 (West Conshohocken, PA: ASTM International, approved May 1, 2020), http://doi.org/10.1520/E0119-20
32. L. E. Hasburgh, K. J. Bourne, D. S. Stone, and S. L. Zelinka, "Simulating Real Compartment Fire Conditions in a Furnace," *Fire and Materials* 44, no. 3 (2020): 333–340.
33. J. Schindelin, I. Arganda-Carreras, E. Frise, V. Kaynig, M. Longair, T. Pietzsch, S. Preibisch et al., "Fiji: An Open-Source Platform for Biological-Image Analysis," *Nature Methods* 9, no. 7 (2012): 676–682.
34. K. Ronewicz, J. Kluska, Ł. Heda, and D. Kardaś, "Chemical and Physical Properties of Pine Wood during Pyrolysis," *Drvna industrija: Znanstveni časopis za pitanja drvne tehnologije* 68, no. 1 (2017): 29–36.
35. W. Kharrat, A. Koubaa, M. Khlif, and C. Bradai, "Intra-Ring Wood Density and Dynamic Modulus of Elasticity Profiles for Black Spruce and Jack Pine from X-Ray Densitometry and Ultrasonic Wave Velocity Measurement," *Forests* 10, no. 7 (2019): 569–584, https://doi.org/10.3390/f10070569